Journal of the Korean Nuclear Society
Volume 18, Number 1, March 1986

SNU 1.5MV Van de Graaff Accelerator (IV)

—Fabrication and Aberration Analysis of Magnetic Quadrupole Lens—

H.I. Bak
Seoul National University

B.H. Choi and H.D. Choi
Korea Advanced Energy Research Institute

(Received November 5, 1985)

SNU 1.5MV 반데그라프 가속기 (IV)

—자기 4극 렌즈의 제작과 수차의 분석—

박 혜 일
서울대학교

최 병 호·최 희 동
한국에너지연구소

(1985. 11. 5 접수)

Abstract

A magnetic quadrupole doublet was fabricated for use at the pre-target position of SNU 1.5MV Van de Graaff accelerator and then its optical characteristics were measured and analysed. The physical dimensions are: pole length 180mm, aperture radius 25mm, pole tip radius 28.75mm. Material for poles and return yokes is carbon steel KS-SM40C. Coils have 480 turns per one pole and air-cooling is adopted. Applying the d.c. current 2.99±0.03A to the lens, and using the Hall probe, magnetic field elements B_θ, B_r were measured at the selected points along each coordinate direction r, θ, z. From the area integration and orthogonal polynomial fitting for the measured data, the magnetic field gradient G=566.3±2.1 gauss/cm at lens center, the effective length L=208.3±1.44mm along the lens axis have been obtained.

The harmonic contents were determined up to 20-pole from the generalised least squares fitting. The results indicate that sextupole/quadrupole is below 1.4±0.9% and all the other multipoles are below 0.5% in the region within 18mm radius at the center of lens.

요 약

SNU 1.5MV 반데그라프 가속기의 표적상자 전단에서 사용될 자기 4극 렌즈를 제작하고 그 광학적 특성을 측정 및 분석하였다. 렌즈의 칫수는 자극 길이 180mm, 구경 반경 25mm, 자극편 반경 28.75mm이며 자극과 철심의 재료로는 탄소강 KS-SM40C를 사용하였다. 코일은 자극 당 480회 감아 공냉식을 채택하고 있다. 제작한 렌즈에 직류 전류 2.99±0.03A를 흘리며 Hall 탐침소자를 써서 r, θ, z의 각 방향에 대해 여러 지점에서 자장 요소 B_θ, B_r을 측정하였다. 측정된 자료에 대한 면적적

분과 직교성 다항함수 fitting을 통하여 렌즈 중심에서 자장 구배 G=566.3±2.1gauss/cm, 렌즈축 상에서 유효길이 L=208.3±1.44mm로 나타났다.

렌즈의 다극 요소는 최소자승법을 써서 20극까지 결정하였다. 결과로서 렌즈 중심의 18mm 반경 이내의 영역에서 6극 요소 대 4극 요소의 비는 1.4±0.9% 이하이고, 기타 다극 요소들은 모두 0.5% 미만임을 얻었다.

1. Definition of Field Components

The principles of magnetic quadrupole lens as a kind of optical components used for ion beam transport is well-known[1], so this study concerns about fabrication of the lens which will be used as a doublet at the pre-target position of SNU 1.5MV tandem Van de Graaff accelerator and also about the measurement and analysis of its optical characteristics.

The magnetic quadrupole with pole shape of exact hyperbola has its magnetic field component as

$$B_x=Gy,\ B_y=Gx. \tag{1}$$

The magnetic potential is given as

$$V=-Gxy,\ G=\mu_0(2nI/a^2) \tag{2}$$

where G is the magnetic field gradient, nI is the number of exciting ampere-turns per pole, a is the lens aperture radius. In practise, it is impossibleto make an exact hyperbola pole. This causes the effective length of lens to vary as position and the magnetic field to have extraneous multipole components other than quadrupole component. To define these terms, $(r,\ \theta)$ coordinate system is introduced as Fig. 1, where x-axis denotes horizontal plane, y-axis vertical plane, z-axis quadrupole lens axis.

The tangential field B_θ is expressed as

$$B_\theta(r,\theta,z)=\sum_{n=1}h_n(r,z)\,(r/a)^{n-1}\cos(n\theta+\delta_n) \tag{3}$$

where a is the aperture radius, h_n is the multipole field coefficient of order n and nearly independent of both r and z inside the fringing field region.

The radial field B_r is given as

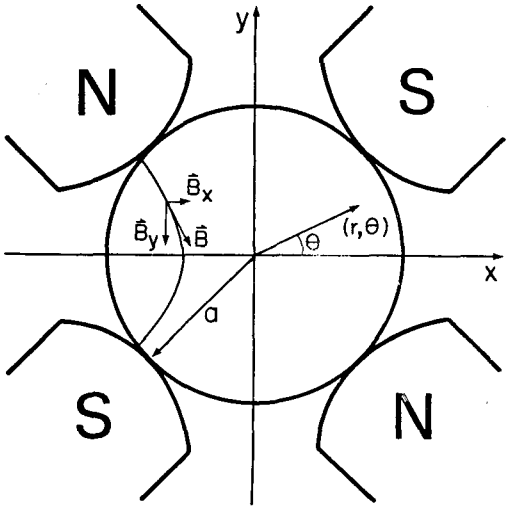

Fig. 1. Coordinate Setting for the Magnetic Quadrupole

$$B_r(r,\theta,z)=\sum_{n=1}k_n(r,z)\,(r/a)^{n-1}\sin(n\theta+\delta_n) \tag{4}$$

and from the fact $\vec{\nabla}\times\vec{B}=0$, $k_n(r,z)=h_n(r,z)+(r/n)(\partial h_n/\partial r)$. Inside the fringing field region, h_n is independent of r and z, so this leads to $h_n=k_n$. The harmonic content of n-th multipole is defined as ratio(%) to quadrupole component,

$$H_n(r/a,z)=(h_n/h_2)\,(r/a)^{n-2} \tag{5}$$

$$K_n(r/a,z)=(k_n/k_2)\,(r/a)^{n-2}. \tag{6}$$

There remains only quadrupole ($n=2$) term for infinite pole shape of hyperbola, but fabrication difficulties make pole cross section finite. Such a case, H_6(12-pole), H_{10}(20-pole), H_{14}(28-pole),... elements exist. Furthermore, when the exact symmetry of 4 poles is not achieved, representative H_3(sextupole), H_4(octapole),... elements exist.

The magnetic field gradient can also be expressed as

$$G_h(r/a,\ z)=\partial B_\theta(r,0,z)/\partial r \quad (7)$$

$$G_k(r/a,\ z)=\partial B_r(r,\pi/4,z)/\partial r \quad (8)$$

and a measure of optical focusing power is defined as

$$P_h(r/a)=\int_{-c}^{c}G_h(r/a,z)\,dz = \frac{\partial}{\partial r}\int_{-c}^{c}B_\theta(r,0,z)\,dz \quad (9)$$

$$P_k(r/a)=\int_{-c}^{c}G_k(r/a,z)\,dz = \frac{\partial}{\partial r}\int_{-c}^{c}B_r(r,\pi/4,z)\,dz \quad (10)$$

where $z=\pm c$ denotes field clamp position but this analysis takes it for $\pm$14cm.

The lens effective length is

$$L_h(r/a)=P_h(r/a)/G_h(r/a,0) \quad (11)$$

$$L_k(r/a)=P_k(r/a)/G_k(r/a,0) \quad (12)$$

as usually defined.

2. Design Procedure

To design the physical dimension and optical parameters of the lens, input data such as particle mass, energy, charge which are accelerator design constraints and various effective lengths, gap length, aperture radius, magnetic excitation of the quadrupole lens have been used for computer program BOTDM[2] which is based on matrix formalism. From the result of program output, suitable object distance and image distance for slit-target distance—a spatial constraint of installation environment have been determined and other lens parameters satisfying stigmatic operation condition, determined as well.

Circular pole shape was adopted for convenience of fabrication. The radius was 1.15 times the aperture radius a to make 12-pole component disappear. Consideration of available space on lens cross section determined magnetic excitation and coil cross section. And then, coil turns, coil length per pole, resistance, maximum operating current, power consumption were determined with the use of available coil current density. These data are shown in Table 1. In Fig. 2, is shown the cross section of the magnetic

Table 1. The Lens Parameters

1. Physical Dimension	
pole length (L_0)	180mm
gap length	160mm
aperture radius (a)	25mm
pole tip radius	28.75mm
width, height	280×280mm
weight	100kg
2. Coil Characteristics	
operating magnetic field	2400 gauss (at pole surface)
operating magnetic excitation	2387 AT* (per pole)
turns per coil	480 turns
operating current	4.97A
maximum supplying current	6.57A
resistance per coil	2.1 ohms
operating power consumption	207.5W (per singlet)
3. Optical Parameters	
object and image distances for	36.1cm (for 3 MeV proton)
stigmatic operation	57.8cm (for 3 MeV deuteron)

*) AT=Ampere-Turns.

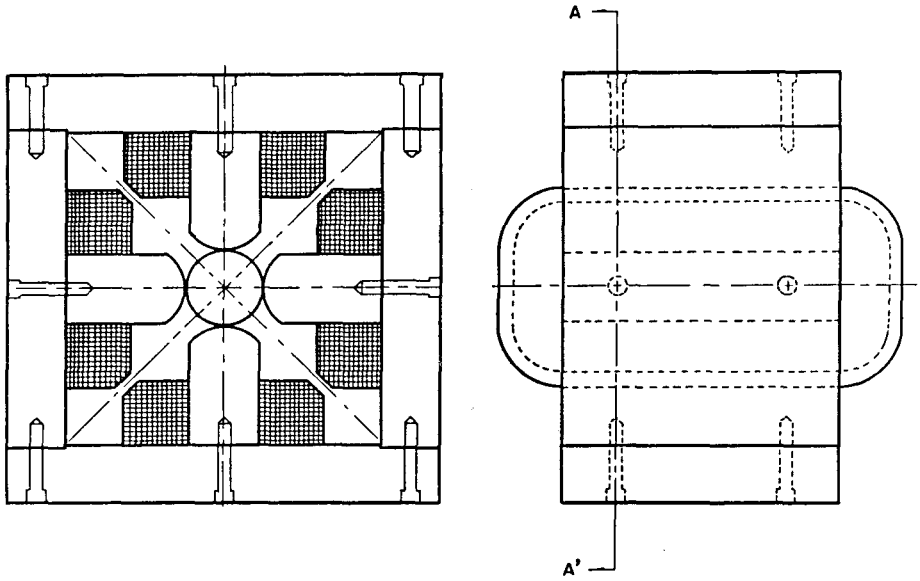

Fig. 2. The Cross Sectional View of the Magnetic Quadrupole Lens

quadrupole lens designed and fabricated.

3. Fabrication

For pole material it is best to use low carbon steel having large magnetic permeability and to test material homogeneity, problems of ordering and material testing in domestic market, however, led all poles and return yokes to be made of carbon steel KS-SM40C. Poles with 28.75mm tip radius were lathe worked, then shaped and polished with 45mm height, 45mm width. These pole tip components were unioned with the lower part of pole prepared by similar procedures. The applied epoxy system was CIBA-GEIGY Araldite AW106 resin/HV953U hardener. Coil was wound with enameled copper wire 1PEW 1.8mmϕ which was generally used for magnet coil. The cross section of coils is shown in Fig. 2. Interlayer gaps and surface of the coils were filled with the previously mentioned epoxy for insulation purpose as well. That coil was cured in usual room environment. As a cooling method for coil, air-cooling using a fan was adopted considering the power consumption. Al-plate was set on the coil to achieve position fixing, easy removal and reassembly of coils. Each Al-plate has inclined edges to fix coils when it contacts each other's edge by assembling the lens. During the procedure of assembling each component, care and rearrangement were paid to keep error from assembly below 0.1mm, i.e., those of pole-to-pole length, inner wall-to-wall length of return yoke. This helped to achieve the pole symmetry.

4. Field Measurement and Data Analysis

Measurements of B_θ and B_r components at various selected points for each coordinate r, θ, z were needed to determine the magnetic field gradient, optical focusing power, effective length of the fabricated lens. So the lens was installed on Mitutoyo surface plate (1m×1m) having an attached xyz coordinate measuring machine. A magnetic Hall probe (element area 2.5mm×1.0 mm by visual estimation) was fixed on the coordinate measuring machine and the lens was aligned so that z-axis was coincident with the

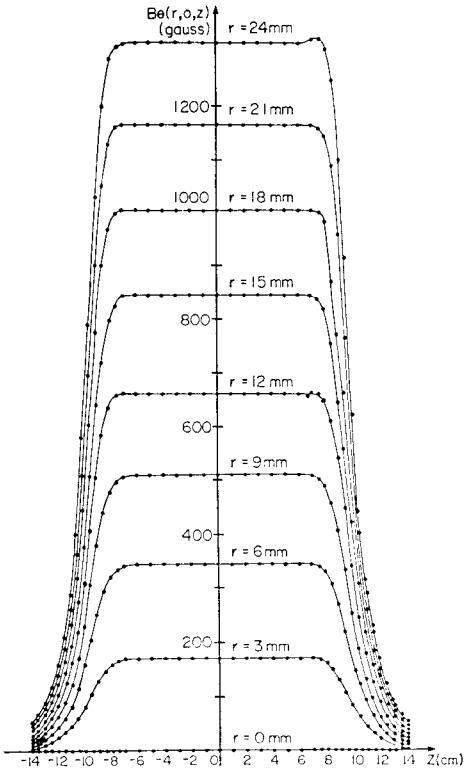

Fig. 3. Measured Data $B_\theta(r, 0, z)$ vs. z

geometric axis of quadrupole lens. Coils were lined in series and applied d.c. 2.99 ± 0.03A with regulated current supply.

On the z-axis, at 1cm intervals between $z=-14$cm and 14cm in order to include at least 95% of the fringing field, and at 3mm intervals on r-axis, B_θ component and B_r component were measured on $\theta=0$ plane and $\theta=\pi/4$ plane, respectively. The measured data are shown on Fig. 3 and Fig. 4. The coordinates used is that shown on Fig. 1. The origin of z-axis is the center of lens and $z=\pm9$cm position is at the edge of pole. An unusual variation of field magnitude around the pole edge at $z=9$cm, as shown on both figures, is expected to be caused from material inhomogeneity and/or fabrication failure during the lathe working of pole edge, but more probably from the latter cause.

Fig. 5 shows the variation of B_θ component on r at $z=0$, ±9cm position of $\theta=0°$ plane.

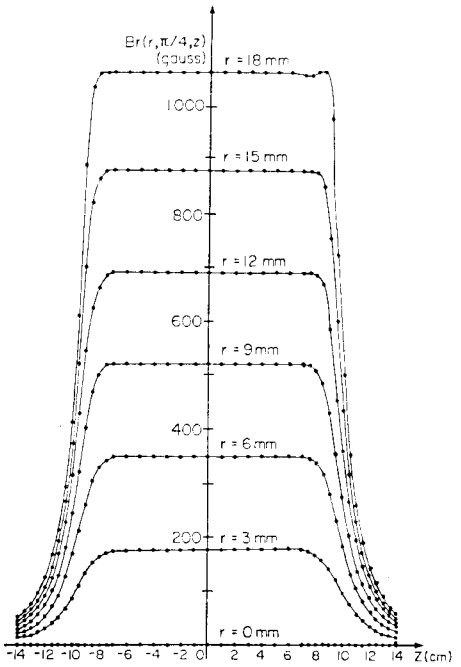

Fig. 4. Measured Data $B_r(r,\pi/4, z)$ vs. z

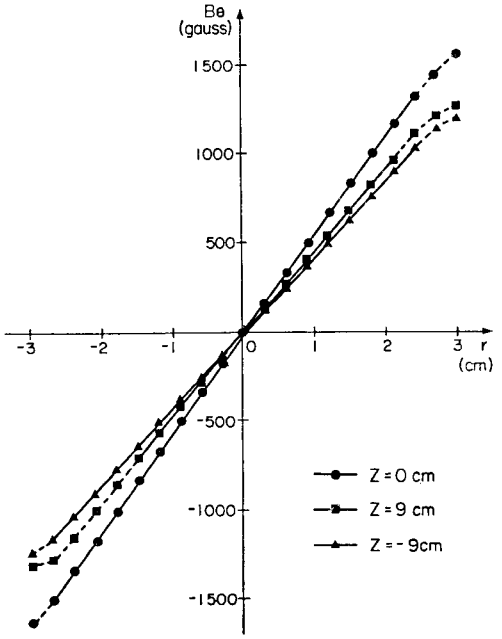

Fig 5. Measured Data $B_\theta(r, 0, z)$ vs. r

Those locations of $r<0$ in the figure mean they are on $\theta=180°$ plane. Measured data $B_\theta(r, 0, z)$ and $B_r(r,\pi/4, z)$ were integrated using a numerical area integration method. The obtained

Table 2. Measure of Optical Focusing Power

1. $\int_{-c}^{c} B_\theta(r, 0, z)dz = \omega_0 + \omega_1(r/a)$

$\omega_0 = 165.99 \pm 48.72$ (gauss·cm)

$\omega_1 = 29494.23 \pm 173.96$ (gauss·cm)

$P_k(r/a) = \frac{\partial}{\partial r}\int_{-c}^{c} B_\theta(r, 0, z)dz$

$= 11797.69 \pm 69.58$ (gauss)

2. $\int_{-c}^{c} B_r(r, \pi/4, z)dz = \omega_0 + \omega_1(r/a)$

$\omega_0 = 105.95 \pm 55.38$ (gauss·cm)

$\omega_1 = 31158.82 \pm 227.55$ (gauss·cm)

$P_k(r/a) = \frac{\partial}{\partial r}\int_{-c}^{c} B_r(r, \pi/4, z)dz$

$= 12463.53 \pm 91.02$ (gauss)

Table 3. Magnetic Field Gradient and Effective Length

1. $B_\theta(r/a, 0, 0) = \sum_{n=1}^{8} c_n (r/a)^{n-1}$

n	c_n(gauss)
1	-3.00 ± 0.002
2	1415.64 ± 5.17
3	6.95 ± 12.47
4	-102.20 ± 38.33
5	-13.58 ± 31.40
6	145.54 ± 65.97
7	-3.65 ± 17.56
8	-79.72 ± 30.20

2. $G_k(r/a, 0) = \partial B_\theta(r, 0, 0)/\partial r$

$= \sum_{n=2}^{8} (n-1) c_n (r/a)^{n-2} (1/a)$

3. $G_k(r/a, 0)$ and $L_k(r/a)$

r/a	$G_k(r/a, 0)$ (gauss/cm)	$L_k(r/a)$ (cm)
0	566.32 ± 2.07*	20.83 ± 0.14
0.8	538.93 ± 8.15*	21.89 ± 0.36

*) uncertainty value 1σ taken covariance $\mathrm{cov}(c_j, c_k)$ into consideration.

areas were fitted with orthogonal polynomial funtions so that it was represented as function of r/a. For this fitting, the orthogonal polynomial fitting program of CERN[3] was executed and from the output of statistical analysis, F-values were reviewed to conclude insignificant the terms above 2nd order of r/a on the statistical point of view. From these procedures, a measure of optical focusing power P_k, P_k were obtained by the equations (9) and (10). The results are shown in Table 2. Similar fitting procedures for $B_\theta(r/a, 0, 0)$ data resulted significant coefficients up to 7th power of r/a. Table 3 summarises the magnetic field gradient and effective length obtained from the above fitting and equations (7) and (11). This $G_k(0, 0)$ value is consistent with that value 575.20 ± 5.79 gauss/cm obtained from equation (2). Effective length $L_k(0)$ is also consistent with $L \cong L_0 + a = 20.50$cm (L_0: pole length, a: aperture radius) as generally known[4]. G_k could not be obtained for lack of data points on B_r component.

To determine the harmonic contents of the lens, Hall probe was mounted on a mandrel so that B_θ and B_r components were measured at $z=0$ and $z=9$cm position. The mandrel axis was coincident with the geometric axis of the quadrupole lens. The probe rotated at $\Delta\theta = 5°$ intervals on $r=18$mm ($r/a=0.72$) radius. Fig. 6 and Fig. 7 show the measurements. Instead of the Fourier analysis, a generalised least squares fitting was carried out taking up to 20-

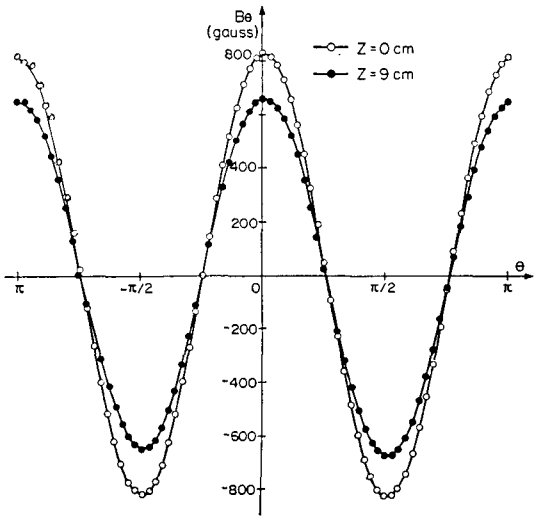

Fig. 6. Measured Data $B_\theta(r/a=0.72, \theta, z)$ vs. θ

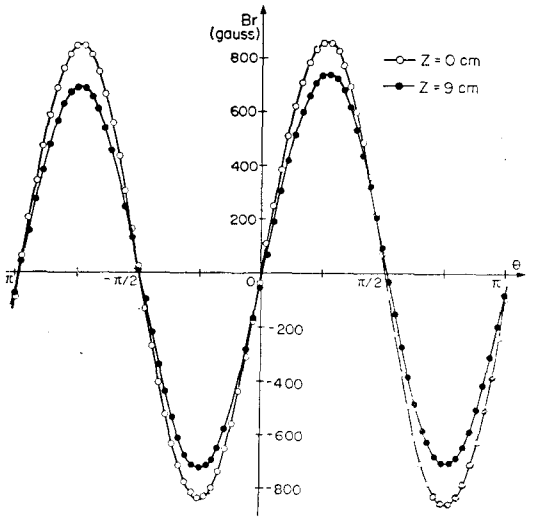

Fig. 7. Measured Data $B_r(r/a=0.72, \theta, z)$ vs. θ

pole into consideration and using the equations (3), (4) for the measured data. This fitting considered those typical systematic errors such as the displacement of the center of probe rotation from the magnetic center and the angle offset error. A FORTRAN subroutine[5] adopting the combined algorithm of gradient search and analytic search was used with the equal unit statistical weight for each input data. The convergence criterion for least squares value, Q^2, was selected below 0.001%. To shorten the computing time, c_n values in table 3 were used as the initial guess values for the multipole components.

The results for h_n—the multipole component at $z=0$ and 9cm position, Δr—the displacement of the center of probe rotation from the magnetic center, and α—the angle offset error, are summarised on Table 4. The phase shift δ_n of multipole component was assumed to be caused dominantly by the angle offset error. Q^2/df on the table denotes the variance of residuals, so its square root value may be considered as the estimated uncertainty of magnetic field magnitude. This is consistent with the uncertainty from the variation of excitation current, 1%. The harmonic content H_n was determined from the definition (5) and shown on Table 5. The fitting for B_r component did not converge to the desired values by some numerical problems but not identified.

Table 4. Multipole Components and Systematic Errors

Data position at $r=1.8$cm, $z=0$cm and 9cm.

h_n (gauss)		center($z=0$cm)	edge($z=9$cm)
dipole	h_1	19.01± 7.11	1.62±22.02
quadrupole	h_2	1138.80± 2.00	920.40± 3.49
sextupole	h_3	−22.23±13.48	−28.80±42.45
octapole	h_4	−11.56± 3.65	−3.03± 6.71
10-pole	h_5	4.17± 5.20	−1.37± 6.33
12-pole	h_6	0.03± 7.36	−27.94± 7.89
14-pole	h_7	5.62± 9.97	10.90±13.17
16-pole	h_8	−5.83±13.56	−7.32±15.00
18-pole	h_9	11.60±19.46	2.56±20.67
20-pole	h_{10}	−39.76±27.34	−2.70±27.61
Δr(cm)*		0.01±0.02	0.01±0.11
α(radian)**		−0.02±0.001	−0.02±0.001
Q^2/df***		73.50	76.82

* The estimated displacement of probe rotation center from the magnetic center.
** The estimated angle offset error.
*** The least squares value per degree of freedom.

Table 5. Harmonic Contents of the Quadrupole Lens

Data position at $r=1.8$cm, $z=0$cm and 9cm.

H_n(%)	center ($z=0$cm)	edge ($z=9$cm)
H_3	1.41 ±0.86	2.25 ±3.32
H_4	0.53 ±0.17	0.17 ±0.38
H_5	0.14 ±0.17	0.055±0.25
H_6	0.0007±0.17	0.82 ±0.23
H_7	0.095 ±0.17	0.23 ±0.28
H_8	0.071 ±0.17	0.11 ±0.23
H_9	0.01 ±0.02	0.03 ±0.23
H_{10}	0.25 ±0.17	0.02 ±0.21

5. Results and Discussions

It turned out that the field gradient is $G_h=$ 566.3±2.1 gauss/cm, the effective length is L_h

$=208.3\pm1.4$mm at the center of lens, $r=0$, $z=0$, under the condition of applied current 2.99 ± 0.03A to quadrupole coil. These values may be concluded to be consistent with the theoretical value or the known approximate value. As shown on Table 5, all multipole components except sextupole are present below 0.5% and sextupole/quadrupole is below 1.4 ± 0.9% in the region between $r=0$ and $r=18$mm at the lens center $z=0$. It is noted that 12-pole component has negligible value, 0.00071%, with respect to its uncertainty, 0.71%. This confirms the validity of design and analysis. The reasons that sextupole is present with the largest value are expected to be machining tolerance, inhomogeneity of material, variation of coil shape and position, fluctuation of operating current in coil. In the fabrication procedure of this lens, inexact pole symmetry from machining inaccuracy seems to be the most serious reason.

When it was in test operation, coil had no heating problem because the measured surface temperature was saturated at 42°C with fan cooling.

6. Conclusions

A quadrupole lens with desired performance could be fabricated and assembled through the design and fabrication procedures previously described. The overall quality of the quadrupole is comparable to the commercial product[6] but there remains some points to be improved in fabrication accuracy and material homogeneity with regard to sextupole component.

The points to be studied later are optical matching with other optical components in SNU 1.5MV VDG accelerator and fixing the operation condition.

The authors wish to recommend to try selecting and testing of the material, lowering the mechanical inaccuracy, tapering the edge of pole to reduce the effect of fringing field, especially for the fabrication of strong focusing lens used for higher energy beam. It is also evident that simplifying the cross section of coil is recommendable for easy fabrication and minimum variation in coil shape.

References

1. E. Regenstreif, "Focusing of Charged Particles," ed. A. Septier, Vol. I, p. 359, Academic Press, New York (1967).
2. K.H. Chung, H.I. Bak et al., *Engineering Report*, Seoul National University, Vol. 16, No. 2, 43 (1984).
3. D.J. Hudson, "Maximum Likelihood and Least Squares Theory," CERN 64-18, p. 173, CERN, Geneva (1964).
4. S. Penner, *Rev. Sci. Instr.*, **32**, 150 (1961).
5. P.R. Bevington, "Data Reduction and Error Analysis for the Physical Sciences," p. 234, Mc-Graw Hill Book Co., New York (1969).
6. ANAC Inc., "Technical Information on Quadrupole Magnets"